

Internal Model Control Scheme for DC-DC Boost Converter

Miss. Madhumati N. Narule¹, Prof. M. C. Butale²

¹Student of Department of Electrical Engineering

² Associate professor of Department of Electrical Engineering
Padmbooshan Vasantraoada Patil Institute of Technology,
Budhgaon

Abstract—This paper presents the design and simulation of a DC-DC Boost converter manipulating IMC and PID controller, enlarging overall performance of the system. The main objective of the DC-DC converter is to keep a constant output voltage even though variations in input/source voltage, components. Designers aim to achieve better conversion efficiency, and better dynamic responses using IMC controller as compared to PID controller dynamic response which improves the output voltage regulation of DC-DC boost converter. A IMC (Internal Model Control) controller instead of a conventional PID (Proportional, Integral and Derivative) controller has been applied to Boost converter and tested in MATLAB-Simulink environment achieving improved voltage regulation. The recommended closed loop implementation of the converter maintains constant output voltage despite changes in input voltage and significantly reduces the problem of tuning of PID and overshoot of response thereby improving the efficiency of the converter. The output of this investigation has the conceivable to accord in a significant way in electric vehicles, industry, communication and renewable energy sectors.

Keywords— DC-DC converter; voltage regulation; Boost converter; dynamics response; open loop boost ;boost with PID; boost with IMC, stability Introduction

1. INTRODUCTION

In the last three decades, there is an increasing demand of switch mode power supplies (SMPS) due to their utilization in the application areas of renewable energy, communication, computers, automobiles, aerospace etc..An improved control of SMPS dynamics can enhance the performance of its end application. Among the various modulation techniques used for SMPS control, PULSE WIDTH-MODULATION (PWM) dc-dc converters are most popular and are used at different power levels. This type of modulated dc-dc converters are advantageous due to their high conversion ratios between input-output, high efficiency and constant frequency of operation. A DC/DC Converter is a static circuit that converts the fixed dc input voltage to a variable a variable DC output voltage directly. A DC - DC converter is considered as it is similar to an dc equivalent of an ac transformer since they behave in an identical manner . As it involves one stage conversion these are more efficient. These are now being used all over the world for rapid transit systems. These are also used in trolley cars, marine hoists, forklift trucks and mine haulers. The electric automobiles are likely to use DC DC converter for their speed control and braking. These offers smooth control, high efficiency, fast response, and regeneration. The power semiconductor

devices used for this converters can be forced commutated thyristors, power BJT, Power MOSFET, GTO, IGBT. In low voltage applications MOSFET is picked over IGBT due to its higher computational speed compared to IGBT. These devices are represented by a switch. When a switch is off no current can flow through it and when it is on the current will flow in particular direction. The power semiconductor devices having on stage voltage drop of 0.5V to 2.5 V across them. For the sake of simplicity this, voltage drop across these devices can be neglected which can be neglected system offers smooth control, high efficiency, fast response and regulation. The three basic nonisolated power electronic circuits are buck, boost and buck boost. Among these configuration a boost converter is widely used in renewable energy applications such as fuel cell, solar PV power conditioning systems here the required output voltage is more than that of input voltage. The main objective in controlling a DC-DC converter is to obtain a desired regulated output voltage in the presence of perturbations change in input voltage. The conventional approach to control a boost type converter is to employ a PID controller. The same system is employed with a IMC controller. The recommended closed loop implementation of the converter maintains constant output voltage despite changes in input voltage and significantly reduces the problem of tuning of PID and overshoot of response thereby improving the efficiency of the converter.

The IMC structure offers an alternate parameterization of the feedback controller (see Fig. 1).The IMC structure offers several advantages over conventional feedback structure:

1. Designing an internal model controller is similar to designing a feed-forward controller, which is much easier than designing the conventional feedback controller.
2. This control structure deal with model-plant mismatch and unmeasured disturbances.
3. Tuning this filter is straightforward when compared to the conventional PID controller.

2. INTERNAL MODEL CONTROL STRUCTURE AND DESIGN PROCEDURE

The IMC design procedure is an capacious and distinct. It has been developed in many forms; these include one-input, one-output (SISO) and multiple input and multiple (MIMO) formulations, continuous-time and discrete-time design procedures, for the unstable open loop system the design

procedures for includes the combined study of feedback-feed forward IMC design, and so forth.

The focus of this is that on the feedback-only SISO design procedure for open-loop stable systems, with appropriate accentuation on its relationship to PID controller tuning. From design point of view of the controller an IMC supports in judging the basic stipulation correlated with feedback control, such as concluding the consequences of zeros present at right half of s-plane on achievable control performance.

Since the finesse of the IMC controller depends on the order of the model as well as requirements of control performance requirements, the IMC design procedure is also applicable in determining when simple feedback control structures (such as PID controllers) are adequate.

The open-loop stable systems are considered in this work. Fig. 1 shows the two-degree-of-freedom IMC (TDOF-IMC) structure, which facilitates separate and simultaneous tuning for the servo and regulatory behaviour of an open loop stable system.

In Fig. 1(a) and 1(b), $p(s)$ represents the plant transfer function, $p\eta(s)$ represents the external disturbance transfer function, $v(s)$ is the measured output and $v_{sp}(s)$ is the set-point. In Fig. 1(a), $p_m(s)$ represents the internal model transfer function, $C(s)$ represents IMC controller, $F_r(s)$ represents the set-point filter and $F\eta(s)$ represents the disturbance filter while in Fig. 1(b), $C_f(s)$ represents the feedback controller.

A distinguishing feature of the IMC structure with reference to the conventional control structure is the use of an internal model in parallel with the plant. Since the model is used in the parallel path, the difference between the model predictions and the measured signal contains explicit information on the MPM and unmeasured disturbances.

Thus, IMC is inherently a predictive structure control scheme. A typical feedback controller design exercise involves shaping the complimentary sensitivity function, which determines the servo performance, and, the sensitivity function, which determines the robustness to the MPM/unmeasured disturbances.

Using the standard rules of block diagram manipulation for closed-loop system shown in Fig1. The equation can be written as follows

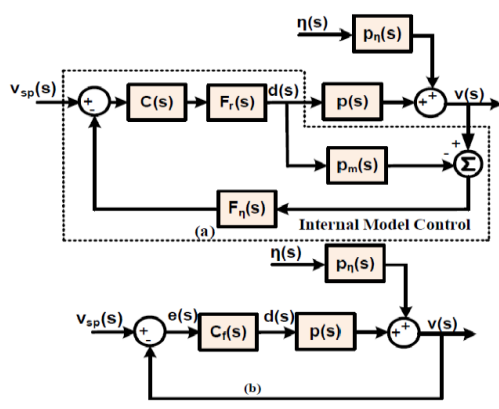


Fig. 1:- (a) Schematic representation of an Internal Model Control Structure
(b) Conventional feedback control structure

$$V(s) = \left[\frac{p(s) C(s) Fr(s)}{1 + C(s) Fr(s) Fn(S) [p(s) - P_m(s)]} \right] V_{sp}(s) + \left[\frac{1 - C(s) Fr(s) Fn(s) p(s)}{1 + C(s) Fr(s) Fn(S) [p(s) - P_m(s)]} \right] p\eta(s) \eta(s) \quad \dots \dots (1)$$

$$\text{Or } v(s) = T(s) v_{sp}(s) + S(s) p\eta(s) \eta(s) \quad \dots \dots (2)$$

where $T(s)$ represents the complementary sensitivity function and $S(s)$ represents the sensitivity function for the IMC structure. In the absence of the MPM, i.e. when $p(s) = p_m(s)$,

$$S(s) = 1 - C(s) Fr(s) Fn(s) p_m(s) \text{ and} \quad \dots \dots (3)$$

$$T(s) = p(s) C(s) Fr(s) \quad \dots \dots (4)$$

It may be noted that, in contrast to the nominal sensitivity functions of the conventional feedback control scheme, the controller appears linearly in the respective sensitivity functions in the IMC strategy. Moreover, two tunable filters, $Fr(s)$ and $F\eta(s)$ are provided in the feedforward and feedback path, respectively. It may be noted that tuning $F\eta(s)$ to shape the nominal sensitivity function does not alter the complementary sensitivity function. Thus, the nominal $S(s)$ and $T(s)$ can be shaped independently in the case of IMC structure.

$$S_f(s) = \left(\frac{1}{1 + Cf(s)p(s)} \right) \cdot p\eta(s) \quad \dots \dots (5)$$

$$T_f(s) = \frac{Cf(s)p(s)}{1 + Cf(s)p(s)} \cdot p\eta(s) \quad \dots \dots (6)$$

On the other hand, in the conventional feedback structure, choosing $C_f(s)$ to shape the nominal $S_f(s)$ alters the $T_f(s)$. As a consequence, it is relatively easy to shape the sensitivity and complementary sensitivity functions for the IMC structure. This implies that the IMC structure provides a better framework for tuning the controller to achieve good performance and robustness simultaneously [20].

A. Some advantages of IMC structure:-

a) *Dual Stability* : In the absence of model-plant mismatch, the closed-loop transfer function reduces to:

$$v(s) = [p(s) C(s) Fr(s)] v_{sp}(s) + [1 - C(s) Fr(s) Fn(s) p(s)] p\eta(s) \eta(s) \quad \dots \dots (7)$$

Thus, if the plant is open loop stable, the nominal closed-loop stability is ensured if the controller is chosen to have stable poles. Through algebraic transformations, any controller in an IMC scheme can be converted to an equivalent conventional feedback controller, $G_c(s)$, using the following relationship [16]:

$$G_c(s) = \frac{C(s) Fr(s) Fn(s)}{1 - P_m(s) C(s) Fr(s) Fn(s)} \quad \dots \dots (8)$$

As can be seen from (8), the IMC structure offers a simple parameterization of all stabilizing controllers $G_c(s)$, in terms of $C(s)$ and $F\eta(s)$ [20].

A major advantage with the IMC structure is that the design procedure and tuning parameters of $C(s)$ and $F\eta(s)$ is relatively easier than the design and tuning of the conventional feedback controller, $C_f(s)$.

(b) *Perfect controller*: For the perfect model scenario, $p(s)=p_m(s)$ and from (1), choosing $C(s)=1/p_m(s)$ is equivalent to achieving the perfect servo response, when no external disturbance is applied.

(c) *Zero Steady-state Offset*: For offset free output response, steady-state gain of the controller must be made equal to the inverse of the steady-state gain of the model. It is straightforward to see a demonstration of this property from equation (7).

B. Design Procedure

In IMC controller design, inverse of the linear perturbation model developed is used to shape the servo response. However, a controller of the form $C(s)=(p_m^-(s))^{-1}$ may not be realizable. In particular, for a non-minimum phase system (with time delays and/or RHP zeros), when model inverse is used in controller design, it produces a physically unrealizable controller. Therefore, to achieve the ideal performance through 'perfect control' is not possible in practice due to the limitations arising from RHP zero. To avoid this problem, the model is factorized into invertible and non-invertible components [16]. Let the model be expressed as

$$P_m(s) = P_m^+(s) P_m^-(s) \quad \dots \dots \dots (9)$$

where $P_m^-(s)$ represents the minimum phase component consisting of all poles and zeros in the left half s-plane and $P_m^+(s)$ represents the non-invertible part that include RHP zeros and time delay. This decomposition is carried out in such a way that $P_m^+(0) = 1$. To make the controller realizable and provide a handle to shape the servo response, the controller is cascaded with a low-pass filter, $F_r(s)$ to ensure that $C(s) F_r(s)$ becomes proper, i.e.

$$C(s) F_r(s) = (P_m^-(s))^{-1} F_r(s) \quad \dots \dots \dots (10)$$

Here, $F_r(s)$ is typically chosen as

$$F_r(s) = \frac{1}{(\lambda r + 1)^n} \quad \dots \dots \dots (11)$$

such that n equals the relative order of the minimum phase part of the plant model and λr is the tuning parameter. With this choice, equation (7) reduces to:

$$v(s) = [P_m^+(s) F_r(s)] v_{sp}(s) + [1 - P_m^+(s) F_r(s) F\eta(s)] p\eta(s) \eta(s) \quad \dots \dots \dots (12)$$

It may be noted that the non-minimum phase component of the plant model $P^+m(s)$ presents an inherent constraint on achievable control quality and cannot be neutralized by any control law. Equation (12) clearly demonstrates that, for no plant/model mismatch case, the speed of set-point response can be shaped directly through appropriately selecting $F_r(s)$. The design of controller $C(s)$ depends on the method used for factorizing the model. It may be noted that the factorization is not unique and can be carried out based on either Integral Absolute Error (IAE) or Integral Square Error (ISE) performance indices for step changes in set-point and disturbance [19].

IMC-IAE Design: This method corresponds to the design of $C(s)$ using the Integral Absolute Error (IAE) criterion, i.e.

$$IAE = \int_0^{T_s} |v_{sp}(t) - v(t)| dt \quad \dots \dots \dots (13)$$

where, T_s is settling time. For step inputs in set-point and disturbances, the factorization (14) minimizes the IAE is

$$P_m^+(s) = \prod_i (-\beta_i s + 1) \quad Re(\beta_i) > 0 \quad \dots \dots \dots (14)$$

The complementary sensitivity function in case of IAE factorization reduces to

$$T_{IAE}(s) = \frac{\prod_i (-\beta_i s + 1)}{(\lambda r s + 1)^n} \quad \dots \dots \dots (15)$$

IMC-ISE Design : This approach corresponds to the design of $C(s)$ using the Integral Square Error (ISE) criterion, i.e.

$$ISE = \int_0^{T_s} (v_{sp}(t) - v(t))^2 dt \quad \dots \dots \dots (16)$$

where, T_s is settling time. For step inputs in set-point and disturbances, the factorization (17) minimizes the ISE is

$$P_m^+(s) = \prod_i \frac{-\beta_i s + 1}{\beta_i s + 1} \quad Re(\beta_i) > 0 \quad \dots \dots \dots (17)$$

It may be noted that the LHP poles have been added as an image of RHP zero to the closed-loop in the all pass factorization (17). With ISE factorization of plant model, the complementary sensitivity function is reduced to

$$T_{ISE}(s) = \prod_i \frac{-\beta_i s + 1}{\beta_i s + 1} \frac{1}{(\lambda r + 1)^n} \quad \dots \dots \dots (18)$$

In this work, both IAE and ISE designs have been considered for factorization of plant model. In addition to choosing controller $C(s)$, the TDOF-IMC controller design involves choosing filter,

$F_r(s)$, in the feed-forward path and designing the MPM/disturbance filter $F\eta(s)$ in the feedback path.

In the absence of MPM and external disturbances, $F_r(s)$ decides the servo behaviour of the closed-loop system. If $F_r(s)$ is chosen as given by equation (11), then tuning reduces to selecting λr such that the servo response is as desired. The filter, $F\eta(s)$ in the feedback path is designed for attaining effective disturbance rejection as follows [20]:

$$F\eta(s) = \frac{\sum_{m=0}^{\infty} s^m}{(\lambda d s + 1)^m} \quad \dots \dots \dots (19)$$

where $\alpha_0=1$, λ_d is a disturbance filter tuning parameter, and m is the number of poles in disturbance transfer function $P_\eta(s)$. The choice of the filter parameter λ_d depends on the allowable noise amplification. The disturbance filter tuning parameter, λ_d can be tuned such that noise amplification criterion, i.e., maximum of $|C(jw)F_r(jw)F_\eta(jw)/C(0)F_r(0)F_\eta(0)| \forall w$, is less than a factor of 20 [20]. The values of the tuning filter parameters (λ_r, λ_d) and α_i appearing in equation (19) can be found by solving for

$$[1 - C(s) F_r(s) F_{\eta}(s) p_m(s)]|_{s=\frac{-1}{\tau_i}} = 0 \quad \dots(20)$$

where τ_i is the distinct time constant associated with the i th pole of $P\eta(s)$.

3. SYSTEM DESCRIPTION AND CONTROL DESIGN

In this section, the feasibility of employing IMC to control the output voltage of a boost type dc-dc converter is investigated. The power stage circuit diagram of the boost type dc-dc converter is shown in Fig. 2.

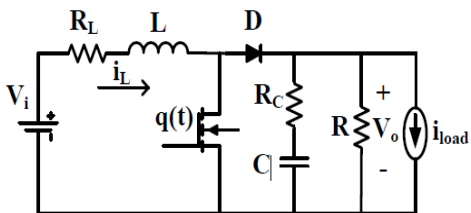


Fig. 2. Power stage circuit diagram of the boost type dc-dc converter.

Table.1:-Specifications of the boost type dc-dc converter

Description	Parameter	Values
Input voltage	V_{in} (V)	10
Capacitance	C (μ F)	1930
Capacitor ESR	$R_c(\Omega)$	0.08
Inductance	L (mH)	3.1
Inductor ESR	$R_L(\Omega)$	0.3
Switching frequency	F_s (kHz)	25
Load resistance (nominal load)	R (Ω)	90
Load resistance (change 50%)	$R/2$ (Ω)	45
Output voltage	V_o (V)	15
Sensing factor	β	1/10
Duty Ratio	D	0.33
Averaged equivalent parasitic resistance	R_{eq}	0.36

$$\begin{bmatrix} \frac{dL(t)}{dt} \\ \frac{dvc}{dt} \end{bmatrix} = \begin{bmatrix} \frac{-Req}{L} & \frac{(1-q(t))RRC}{(R+RC)L} & \frac{(1-q(t))R}{(R+RC)L} \\ \frac{(1-q(t))R}{(R+RC)C} & -\frac{1}{(R+RC)C} \end{bmatrix} \begin{bmatrix} iL(t) \\ vc(t) \end{bmatrix} + \begin{bmatrix} \frac{1}{L} & \frac{(1-q(t))RRC}{(R+RC)L} \\ 0 & \frac{R}{(R+RC)C} \end{bmatrix} \begin{bmatrix} vi(t) \\ iload(t) \end{bmatrix} \quad \dots \dots \dots (21)$$

The Control input $q(t)$ takes a value in the discrete set $\{0,1\}$ switch position function either ON or OFF. In many power electronic circuits , average values of voltages and currents are important rather than their instantaneous values [34].]. In power electronic converters, the average value of switching function $q(t)$ corresponds to the duty ratio of the converter, i.e. in pulse width modulation implementation; duty ratio function $d(t)$ represents the average control input or the control effort which is restricted in the closed interval $[0, 1]$. The state-space averaged model [35, 36] of boost type dc-dc converter in CCM can be obtained by replacing $q(t)$ with $d(t)$. In equation (21), $iL(t)$, $Vc(t)$ represents the inductor current and output capacitor voltage. The system parameters are comprised by L and C which are input circuit inductance and output filter capacitance respectively, while R represents load resistance, subjected to vary. Rc and RL represents the parasitic of capacitor and inductor From the control viewpoint, the external voltage source, $vi(t)$, and load current, $i_{load}(t)$, represent the disturbance inputs The controlled variable is output voltage $vo(t)$.

A. *The objective of closed-loop control system is twofold here.*

a) *Regulatory control problem:* Maintain constant output voltage V_o in the presence of input voltage changes and load disturbances.

(b) *Servo control problem:* Tracking the desired set-point voltage $v_{sp}(t)$ which is higher than the source voltage V_i . Defining perturbation signals, $\tilde{i}_L(t) = i_L(t) - I_L$, $\tilde{V}_C(t) = v_C(t) - V_C$, $\tilde{v}_i(t) = v_i(t) - V_i$, $\tilde{d}(t) = d(t) - D$, where the uppercase letters indicates the corresponding nominal steady state values, and taking Laplace transform of the resulting linear state-space model, the corresponding control-to-output transfer function, line-to-output transfer function and output impedance transfer function can be obtained as follows:

$$P_m(s) = \frac{\bar{v}o(s)}{\bar{d}(s)} = \frac{V_o}{1 - D} \frac{(1 + CRCs)[R^2 + (1 - D)^2 - (R + R_c)(Req + Ls)]}{den(s)} \dots \dots (22)$$

where $\text{den}(s) = R(1 - D)[R(1 - D) + RC(1 + C(R + RC)s)] + (R + RC)(Req + Ls)(1 + C(R + RC)s)$

Specifications of the boost type dc-dc converter used for this study are reported in Table 1. For the values specified in Table 1, we have

$$P_m(s) = \frac{22.0617(1.544 \times 10^4 s + 1)(-7.8287 \times 10^5 s + 1)}{1.3345 \times 10^{-5} s^2 + 1.8847 \times 10^{-3} s + 1} \quad \dots \dots \dots (23)$$

Equation (23) shows the presence of RHP-zero, an LHP-zero and a complex-conjugate pole pair. The linear equivalent circuit of the boost converter shown in Fig. 2 contains a single-section of L-C low-pass filter and the corner frequency, w_0 of this filter is given by:

$$W_0 = \frac{1-D}{\sqrt{LC}} = 272.5 \text{ rad/s} \quad \dots \dots \dots (24)$$

and the position of RHP zero is given as

$$WRHP = \frac{R^2(1-D)^2}{(R+RC)L} - \frac{R_{\text{req}}}{L} = 12.273 \text{ krad/s} \quad \dots \dots \dots (25)$$

Equations (24) and (25) show that both w_0 and $WRHP$ are the functions of the nominal duty cycle (D).

The converter line-to-output transfer function is given as:

$$\frac{\tilde{v}_o(s)}{\tilde{v}_i(s)} = \frac{(1 + CRCs)(1 - D)R(R + RC)}{\text{den}(s)} \quad \dots \dots \dots (26)$$

and the converter output impedance transfer function is given as:

$$\frac{\tilde{v}_o(s)}{-i_{\text{load}}(s)} = \frac{\text{num load}(s)}{\text{den}(s)} \quad \dots \dots \dots (27)$$

where, $\text{num load}(s) = (1 + CRCs)R \times [R(1 - D)Rc - R(1 - D)^2 Rc + (R + RC)(R_{\text{req}} + Ls)]$

In particular, for the system under consideration, we have

$$\frac{\tilde{v}_o(s)}{\tilde{v}_i(s)} = \frac{1.486(1.544 \times 10^{-4}s + 1)}{1.3345 \times 10^{-5}s^2 + 1.8847 \times 10^{-3}s + 1} \quad \dots \dots \dots (28)$$

$$\frac{\tilde{v}_o(s)}{-i_{\text{load}}(s)} = -\frac{0.8567(1.544 \times 10^{-4}s + 1)(8.0639 \times 10^{-3}s + 1)}{1.3345 \times 10^{-5}s^2 + 1.8847 \times 10^{-3}s + 1} \quad \dots \dots \dots (29)$$

Equations (28) and (29) shows that the dynamics of input voltage and load current variations affects the of output voltage in the same way as the control signal.

B. Design requirements for controllers:

The controllers for the closed-loop system will be designed with the following steady state and dynamic requirements for the disturbance rejection and set-point change cases.

(a) *Steady state specification for regulatory and servo response:*

The steady state error in output voltage must be less than 1% of the nominal desired output voltage.

(b) *Transient specification for input voltage change:*

Ensuring stability for changes in the input voltage, $10V \pm 30\%$ variation and the overshoot/undershoot should not be more than $\pm 10\%$ of the nominal output voltage (13.5-16.5 V).

(c) *Transient specification for load variation:* Ensuring stability for changes in 90Ω to 45Ω (-50%) variation i.e., twice the change in load current.

(d) *Transient specification for servo response:* The overshoot for set-point change must not be more than 10% of the perturbation in set-point.

C. Controller Design:

The IMC procedure involves two designs subjected to the ways of factorizing the plant model of (23) and the designs are as follows.

a) **IMC-IAE Design:** The invertible part of plant model is chosen as

$$p_m^-(s) = \frac{22.0617(1.544 \times 10^{-4}s + 1)}{1.3345 \times 10^{-5}s^2 + 1.8847 \times 10^{-3}s + 1} \quad \dots \dots \dots (30)$$

and the non-invertible part of plant model is chosen as

$$p_m^+(s) = (-7.8287 \times 10^{-5}s + 1) \quad \dots \dots \dots (31)$$

The IMC-IAE controller $C(s)$ takes the form

$$C(s) = \frac{1.3345 \times 10^{-5}s^2 + 1.8847 \times 10^{-3}s + 1}{22.0617(1.544 \times 10^{-4}s + 1)} \quad \dots \dots \dots (32)$$

Based on the expected set-point tracking response for the chosen boost converter, the value of filter tuning parameter, λ_d in the forward path is chosen as 5.5ms. To achieve fast disturbance rejection, choose the disturbance filter $F\eta(s)$ to cancel the poles of (28), (29) takes the form as

$$F\eta(s) = \frac{3.982 \times 10^{-5}s^2 + 8.49 \times 10^{-3}s + 1}{(\lambda_d s + 1)^2} \quad \dots \dots \dots (33)$$

In practical applications, system robustness is more crucial than the nominal performance and as a measure of system robustness, the peak value of sensitivity function (M_s) has been used and is defined as:

$$M_s = \text{Max}_{0 \leq w \leq \infty} |S(jw)| \quad \dots \dots \dots (34)$$

M_s measures the closeness of the Nyquist plot from the critical point (-1, 0) at all frequencies and not just at the two frequency points as associated with gain and phase margins. Normally, M_s varies in the range of 1.2-2.0. To provide fair comparisons, among the IMC designs, filter coefficients were tuned such that M_s turns out to have a value = 1.235, ensuring both controllers has same degree of robustness. Based on this criterion, the parameter of filter in the feedback path was selected as $\lambda_d = 0.8$ ms.

A single filter in the feedback path is sufficient, as the denominator polynomials for both the disturbance transfer functions are indistinguishable.

(b) **IMC-ISE Design :** The invertible part of plant model is chosen as follows

$$p_m^-(s) = \frac{22.0617(1.544 \times 10^{-4}s + 1)(7.8287 \times 10^{-5}s + 1)}{1.3345 \times 10^{-5}s^2 + 1.8847 \times 10^{-3}s + 1} \quad \dots \dots \dots (35)$$

and the non-invertible part of plant model was chosen as

$$p_m^+(s) = \frac{(-7.8287 \times 10^{-5}s + 1)}{(7.8287 \times 10^{-5}s + 1)} \quad \dots \dots \dots (36)$$

The IMC-ISE controller $C(s)$ takes the form

$$C(s) = \frac{(1.3345 \times 10^{-5}s^2 + 1.8847 \times 10^{-3}s + 1)}{22.0617(1.544 \times 10^{-4}s + 1)(7.8287 \times 10^{-5}s + 1)} \quad \dots \dots \dots (37)$$

In this case, tuning parameters, $\lambda_r=5.5\text{ms}$, $\lambda_d=1.23\text{ms}$ were chosen such that IMC design with ISE factorization also turns out have the maximum sensitivity function value = 1.235 and corresponding parameters for filter $F\eta(s)$ are $\alpha_2=4.357\times10^{-5}$, $\alpha_1=6.767\times10^{-3}$.

IV. SIMULATION STUDIES

A simulation studies involves the behavior of the boost converter under three circumstances involving open loop boost converter(Fig.3), a closed loop boost converter using PID controller(Fig.4) and a closed loop boost converter using a Internal Model Controller Scheme(Fig.5) . The simulations were carried out using a nonlinear model developed from Sim Power Systems Toolbox of MATLAB/SIMULINK using the parameters listed in Table 1. A simulation study involves the regulatory behavior of a boost converter in open loop condition(Fig.6) i.e, without any controller ,a behavior with PID controller (Fig.7) and a behavior with IMC controller(Fig.8). After comparing the simulation results of open loop boost and closed loop boost converter with PID it is concluded that the regulatory behavior of closed loop with PID is much better than a response of open loop boost converter.

But the comparative study of boost converter with PID and boost with IMC states that an IMC having a better dynamic response compared with PID as PID is difficult to tune as well as controller performance parameter like maximum peak overshoot/ undershoots, settling time .

On the other hand IMC demands less control efforts and manages the transitions without any input saturation. IMC was found to perform significantly better than a PID controller designed using the conventional approach.

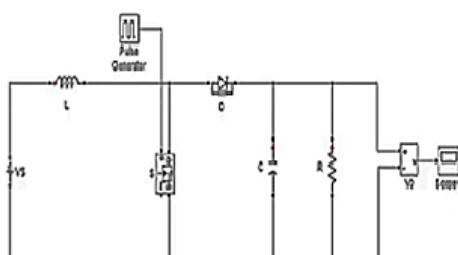


Fig.3. Simulation of Open Loop Boost Converter

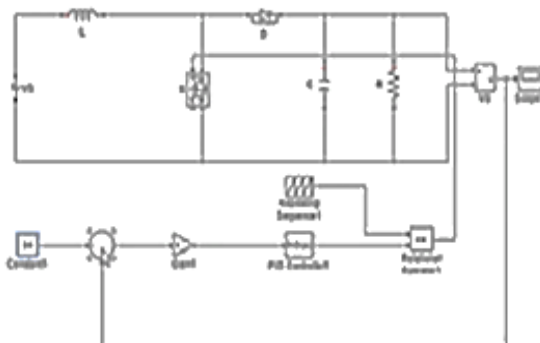


Fig.4. Simulation of Closed Loop Boost Converter with PID controller

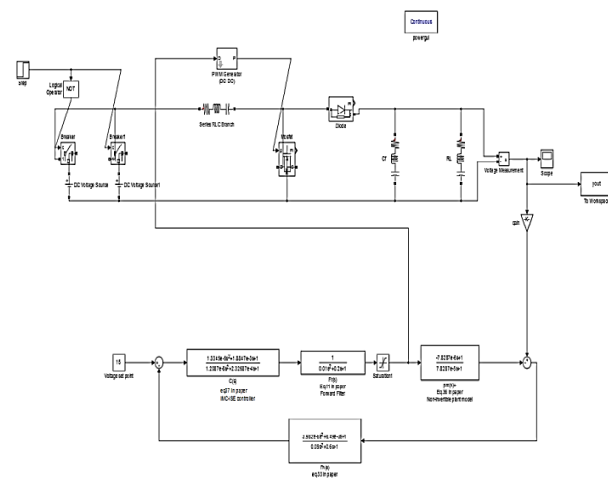


Fig.5. Simulation of Closed Loop Boost Converter with IMC controller

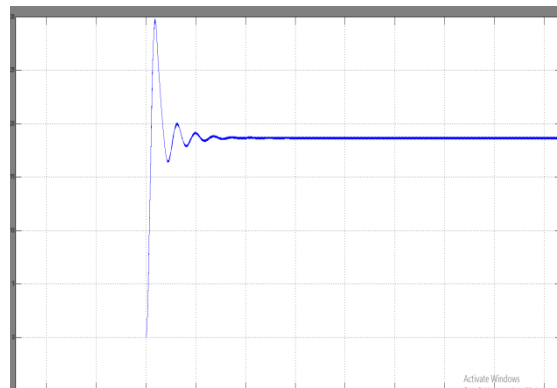


Fig.6. Simulation Result of Open Loop Boost Converter

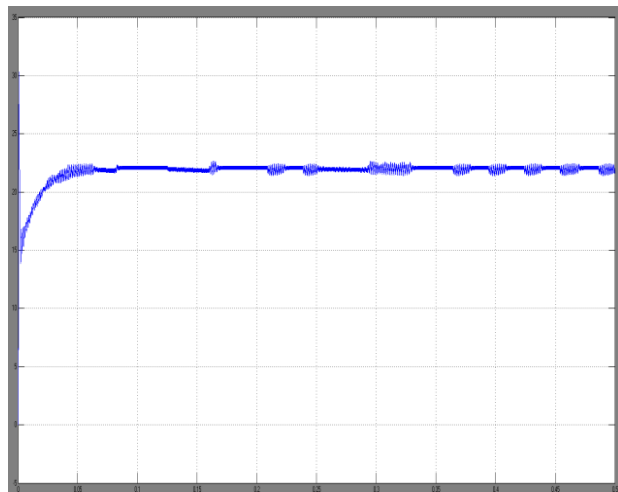


Fig.7. Simulation result of Closed Loop Boost Converter with PID Controller

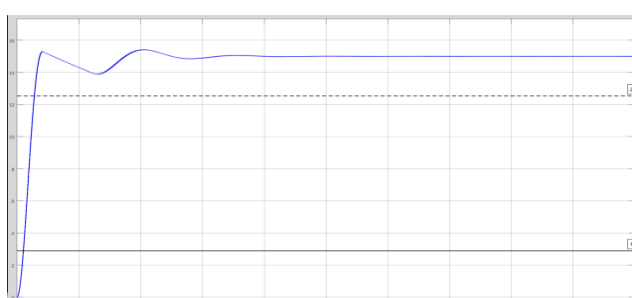


Fig.8. Simulation result of Closed Loop Boost Converter with IMC Controller

5 . CONCLUSION

In this work, an internal model control (IMC) scheme has been implemented as a voltage mode controller for the output voltage regulation of a boost type dc-dc converter operated in CCM. The IMC structure provides a better framework for tuning the controller to achieve good and regulatory performances simultaneously as compared to the PID controller. More importantly, IMC design procedure provides a transparent approach to design a controller that can operate to have a better performance limits. An IMC controller was designed using a linear model developed in the neighborhood of a nominal operating point of the converter. To assess the robustness of the IMC scheme, simulation studies were carried out for a variety of servo and regulatory control scenarios using a nonlinear model for simulating the plant dynamics.

6. REFERENCES

- [1] K. Tarakanath, Sachin Patwardhan, Vivek Agarwal, "Internal Model Control of DC-DC Boost Converter Exhibiting Non-minimum Phase Behavior" 2014 IEEE International Conference on Power Electronics, Drives and Energy Systems (PEDES).
- [2] Truong Nguyen Luan Vu, Le Hieu Giang, Le Linh, and Vo Lam Chuong "Advanced IMC-PID Controller Design for the Disturbance Rejection of First Order Plus Time Delay Processes" 2017 International Conference on System Science and Engineering (ICSSE).
- [3] M H Moradi "New techniques for PID Controller Design" 2003 IEEE.
- [4] Bogdan Doicin, Marian Popescu, Cristian Patrascioiu "PID Controller Optimal Tuning" ECAI 2016 - International Conference – 8th Edition Electronics, Computers and Artificial Intelligence 30 June -02 July, 2016, Ploiesti, ROMÂNIA.
- [5] Kiam Heong Ang, Gregory Chong, Yun Li " PID Control System Analysis, Design, and Technology" IEEE Transactions On Control Systems Technology, Vol. 13, No. 4, July 2005
- [6] Yosra Massaoudi Dorsaf Elleuch Driss Mehdi Tarak Damak and Ghani Hashim "Comparison between Non Linear Controllers Applied to a DC-DC Boost Converter" International Journal of Innovative Computing, Information and Control Volume 11, Number 3, June 2015.
- [7] Hang Wu, Weihua Su, Zhiguo Liu "PID controllers: design and tuning methods" , 2014 IEEE 9th Conference on Industrial Electronics and Applications (ICIEA).
- [8] K. Tarakanath, Sachin Patwardhan, Vivek Agarwal, "Implementation of an Internal Model Controller with Anti-Reset Windup Compensation for Output Voltage Tracking of a Non-Minimum Phase DC-DC Boost Converter using FPGA" ,2016
- [9] D.B. Santosh Kumar, R. Padma Sree, "Tuning of IMC based PID controllers for integrating systems with time delay",2016 ISA.

[10] T.Elakkiya1, R.Priyanka, S.Kiruthika, R.Padma Priya "Comparative study of PID, IMC and IMC based PID controller for pressure process" International Conference on Science, Technology, Engineering & Management Journal of Chemical and Pharmaceutical Sciences ,Issue 10, July 2015.

[11] A. Balestrino, E. Crisostomi, " Advanced PID controllers in MIMO systems" International Symposium on Power Electronics, Electrical Drives, Automation and Motion,2010 IEEE